A Martensite Boundary on the WRC-1992 Diagram — Part 2: The Effect of Manganese

Manganese is found to be more powerful than nickel in stabilizing austenite with respect to transformation to martensite

BY D. J. KOTECKI

ABSTRACT. The upper boundary for martensite appearance in stainless steel weld metals on the Schaeffler Diagram is shown to be overly conservative. It also does not predict a manganese effect beyond its coefficient in the nickel equivalent. A modification to the WRC-1992 Diagram is proposed, which takes variation of manganese into account. The martensite boundary is based upon magnetic measurements and 2T longitudinal face bend tests of numerous submerged arc weld claddings. Separate boundaries are offered for 1%, 4% and 10% Mn.

Introduction

The Schaeffler Diagram (Ref. 1), now fifty years old, is well outdated for ferrite prediction in stainless steel welds. It was supplanted in large part by the DeLong Diagram (Ref. 2), which has in turn been supplanted by the WRC-1992 Diagram (Ref. 3). The newer diagrams make predictions in terms of Ferrite Number (FN) instead of ferrite percent (FP). FN is more reproducible than FP, and it is obtained nondestructively, by magnetic means. Since 1995, the WRC-1992 Diagram has been the recommended method of ferrite prediction in the ASME Code (Ref. 4). However, the WRC-1992 Diagram did not take martensite formation into account. Because the Schaeffler Diagram does make martensite predictions, it tends still to be referenced in stainless steel weld cladding and dissimilar metal joining situations.

Since the WRC-1992 Diagram is recommended for ferrite prediction, it is rather awkward to still rely on the Schaeffler Diagram for martensite prediction. Accordingly, a study was undertaken to allow placement of a martensite boundary on the WRC-1992 Diagram. The first part of this study concentrated on compositions containing nominally 1% Mn, and showed the upper martensite boundary on the Schaeffler Diagram does not agree well with the experimental results (Ref. 5). Using results of magnetic measurements and 2T longitudinal face bend tests, an upper martensite boundary, for 1% Mn compositions, was proposed for the WRC-1992 Diagram.

However, it must be recognized there are a number of stainless steel weld filler metal compositions of appreciably more than 1% Mn content. Such compositions include AWS Type 307 (typically around 4% Mn), the European 18 8 Mn (typically around 6% Mn) and the AWS Type 219 (typically around 10% Mn). These filler metals are often used as cladding or buffer layers, or for dissimilar metal joining. Manganese has been shown to have a negligible effect on solidification of stainless steel weld metals as regards formation of ferrite or austenite at high temperature (Ref. 6). But manganese has a very important effect of stabilizing austenite as regards transformation to martensite at low temperatures (Ref. 7). So it is of interest to extend the earlier work to consider higher Mn levels than 1%, and to examine how higher Mn levels in the weld metal affect the position of the upper martensite boundary on the WRC-1992 Diagram.

KEY WORDS

Stainless Steel
Manganese
Weld Cladding
Martensite
WRC-1992 Diagram
Bend Test

Experimental Materials

Numerous chromium-nickel stainless steel single-pass deposits were produced by submerged arc welding on carbon steel plate. All of the wires employed in Part 2 of this study were 3/32-in. (2.4-mm) diameter tubular metal cored wires. Two series of wires were specially fabricated, one to obtain single-pass deposit compositions on ASTM A36 steel of about 4% Mn, and the second to obtain single-pass deposit compositions of about 10% Mn. The wire compositions were all designed to produce deposits of about 0.1% C, 0.5% Si and 0.02% N, with no significant Mo or Nb content. The compositional variables, then, were Mn, Cr and Ni. Table 1 lists the nominal wire compositions, based upon calculation from the fill formulation. Since dilution from the A36 steel is not taken into account in these calculated wire compositions, and since some loss of manganese during welding was expected, the nominal wire compositions are appreciably higher in Mn than the 4% and 10% targets for the weld deposits. It is the deposit composition that is important.

Only unalloyed high basicity fluxes were used in this part of the study. They are standard commercial products.

Experimental Welds and Evaluation

Each wire was used to make deposits under several welding conditions, primarily varying wire feed speed (current), with corresponding change in travel speed to obtain more-or-less consistent

D. J. KOTECKI is with The Lincoln Electric Co., Cleveland, Ohio.

Table 1 — Calculated Wire Compositions

Wire Number	Calculated Wire Composition (wt-%) C	Mn	P	S	Si	Cr	Ni	Mo	Nb	N
				Wires Producing Diluted Deposits of about 4% Manganese						
1761	0.119	7.65	0.007	0.006	0.06	5.61	11.32	0.00	0.00	0.0004
1762	0.031	8.57	0.015	0.010	0.33	27.39	6.29	0.16	0.00	0.027
1775	0.122	8.57	0.015	0.012	0.30	21.89	10.48	0.16	0.00	0.027
1776	0.109	6.65	0.008	0.008	0.46	7.28	19.63	0.00	0.00	0.0004
1777	0.103	6.64	0.010	0.005	0.58	24.54	2.93	0.00	0.00	0.0004
1786	0.102	7.18	0.008	0.006	0.49	27.55	2.70	0.00	0.00	0.0004
1787	0.111	7.19	0.008	0.009	0.42	7.19	20.71	0.00	0.00	0.0004
1791	0.112	7.72	0.007	0.009	0.41	6.53	22.06	0.00	0.00	0.0004
1792	0.102	7.18	0.008	0.006	0.46	28.76	2.70	0.00	0.00	0.0004
				Wires Producing Diluted Deposits of about 10% Manganese						
1793	0.111	19.28	0.008	0.009	0.41	6.56	9.00	0.00	0.00	0.001
1794	0.110	19.28	0.008	0.008	0.49	14.81	3.65	0.00	0.00	0.001
1795	0.111	19.28	0.007	0.008	0.46	14.90	4.55	0.00	0.00	0.001

weld deposit weight per unit length, but varying dilution so a number of different compositions could be obtained with a single wire. In the early part of the study, weld deposits were stringer beads. Later in the study, 1-in. (25-mm) oscillation was employed to produce a wider deposit that was more easily chemically analyzed by spectrographic methods. In all cases, the base metal was ASTM A36 carbon steel of approximately 0.15% C, ½ in. (12.7 mm) thick and 3 in. (75 mm) wide. The weld deposits were about 14 in. (355 mm) long, so that bending in the longitudinal direction did not include the arc start or crater area. Except for introducing oscillation, the approach is the same as during the first part of the study, as reported in Ref. 5.

Two methods were used to evaluate the presence of martensite in the as-welded condition. The first was a magnetic measurement of "FN" in the as-deposited condition after lightly grinding the weld centerline smooth. "FN" is used in quotation marks here to indicate that, while the instrument is calibrated according to AWS A4.2 for FN measurements, that which is being measured can be ferrite and/or martensite, since both microstructures are ferromagnetic. The measured "FN" was compared with the FN calculated from the WRC-1992 Diagram, extrapolating the iso-ferrite lines in the diagram if necessary. Then the presence of martensite is indicated by the measured "FN" exceeding the calculated FN by more than 1.0. Conversely, the absence of martensite is indicated by the measured "FN" being nearly equal to, or less than, the calculated FN.

The second method used to evaluate the presence of martensite was to perform a longitudinal face bend test around a mandrel whose radius was twice the thickness of the base metal (a test commonly referred to as a "2T" bend test). This test requires at least 20% tensile elongation in the weld metal to pass the test without cracking. A given weld then either passes the test, or it cracks. Cracking is taken to be evidence of martensite, which is brittle, in the as-deposited condition.

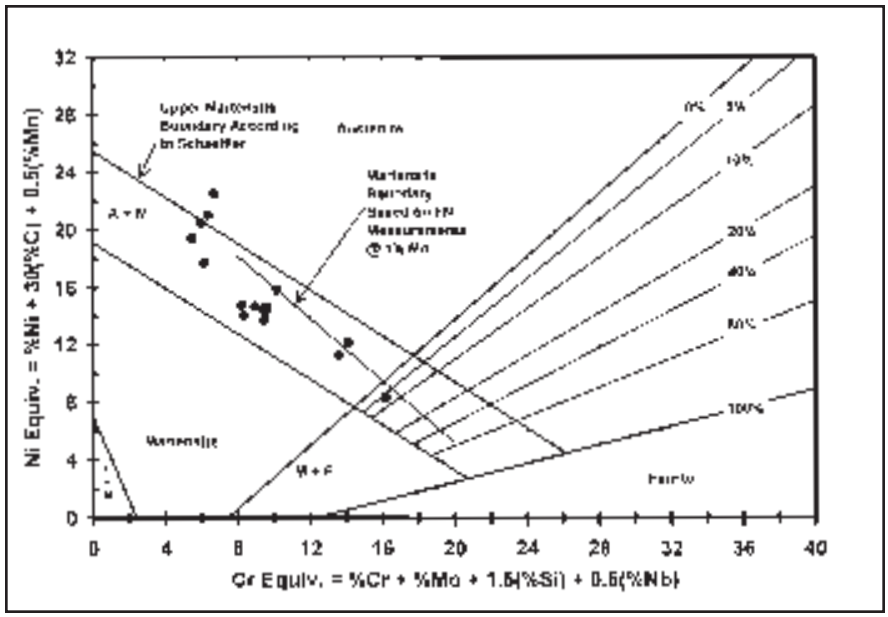

Fig. 1 — Martensite-free 4% Mn compositions on the Schaeffler Diagram. Many 4% Mn compositions, indicated by solid circles, are below the 1% Mn martensite-free boundary.

Metallographic examination had been used in the first part of this study to verify martensite was indeed present in certain samples. Given the excellent correlation of metallographic determinations with magnetic measurements and bend test results, it was not considered necessary to perform more than a few metallographic examinations, and none are reported herein.

After the "FN" measurement and bend test, the sample was bent back flat. Then the region of the apex of the bend was prepared for chemical analysis. Chips were machined for C, S and N by fusion analysis. The remainder of the analysis was performed by optical emission spectrophotometry and/or X-ray fluorescence, with a limited number of wet analyses done also as checks on the spectrographic methods. From the chemical analysis data, chromium and nickel equivalents according to both the Schaeffler and the WRC-1992 Diagrams were calculated. These were then plot-

Table 2 — Experimental Results

Test Weld Number	Deposits Composition, % C	Mn	P	S	Si	Cr	Ni	Mo	Cu	Nb	N	Measure "FN"	WRC FN	Schaeffler % Ferrite
1761-1	0.107	4.80	0.018	0.013	0.34	9.58	10.25	0.10	0.16	N.D.[(a)]	0.022	0.0	0.0	0.0
1761-2	0.106	4.10	0.017	0.015	0.29	8.93	9.31	0.08	0.15	N.D.	0.021	0.0	0.0	0.0
1761-3	0.117	4.05	0.017	0.014	0.25	6.49	9.14	0.10	0.14	N.D.	0.021	0.0	0.0	0.0
1761-4	0.111	3.85	0.017	0.015	0.27	7.87	8.80	0.08	0.15	N.D.	0.021	0.8	0.0	0.0
1761-5	0.117	4.15	0.017	0.015	0.26	7.78	9.20	0.08	0.14	N.D.	0.020	0.4	0.0	0.0
1761-6	0.115	4.00	0.017	0.015	0.25	7.50	8.35	0.08	0.14	N.D.	0.020	2.7	0.0	0.0
1761-7	0.101	3.99	0.016	0.016	0.38	8.80	8.73	0.12	0.16	N.D.	0.021	0.1	0.0	0.0
1761-8	0.110	4.36	0.015	0.015	0.40	8.86	9.19	0.12	0.15	N.D.	0.020	0.0	0.0	0.0
1761-9	0.112	4.39	0.019	0.018	0.49	8.72	8.83	0.13	0.16	N.D.	0.020	0.0	0.0	0.0
1762-1	0.065	4.85	0.023	0.007	0.48	15.45	4.52	0.13	0.18	N.D.	0.044	25.5	6.2	3.9
1762-2	0.064	4.85	0.022	0.010	0.46	16.05	4.23	0.13	0.17	N.D.	0.036	14.7	11.3	7.4
1762-3	0.071	4.55	0.020	0.011	0.44	15.45	3.97	0.12	0.16	N.D.	0.032	8.1	8.9	6.0
1762-4	0.073	4.40	0.019	0.014	0.38	15.38	3.79	0.12	0.16	N.D.	0.031	11.0	9.0	6.1
1762-5	0.075	4.15	0.018	0.011	0.33	14.51	3.64	0.10	0.15	N.D.	0.030	14.4	4.9	2.3
1762-6	0.072	4.20	0.017	0.014	0.56	14.16	3.76	0.13	0.17	N.D.	0.027	11.4	3.6	2.1
1762-7	0.079	4.06	0.020	0.015	0.69	12.56	3.51	0.13	0.17	N.D.	0.025	54.3	0.0	0.0
1775-1	0.102	4.25	0.017	0.019	0.47	11.12	5.77	0.14	0.17	N.D.	0.023	3.1	0.0	0.0
1775-2	0.101	3.90	0.017	0.018	0.47	10.86	5.34	0.12	0.17	N.D.	0.023	36.3	0.0	0.0
1775-3	0.098	3.75	0.018	0.014	0.54	11.61	5.67	0.13	0.17	N.D.	0.024	19.0	0.0	0.0
1775-4	0.108	4.22	0.017	0.016	0.50	10.589	5.53	0.13	0.16	N.D.	0.024	7.4	0.0	0.0
1775-5	0.103	4.84	0.019	0.014	0.67	12.98	6.64	0.15	0.18	N.D.	0.027	0.0	0.0	0.0
1775-6	0.105	3.95	0.019	0.016	0.59	10.75	5.40	0.13	0.17	N.D.	0.024	9.0	0.0	0.0
1775-7	0.099	4.07	0.021	0.014	0.61	11.16	5.63	0.13	0.17	N.D.	0.024	4.2	0.0	0.0
1775-8	0.103	4.45	0.025	0.020	0.85	12.18	5.93	0.15	0.17	N.D.	0.026	0.0	0.0	0.0
1776-1	0.080	3.76	0.021	0.014	0.81	4.90	12.57	0.02	0.05	N.D.	0.010	23.2	0.0	0.0
1776-2	0.092	3.30	0.017	0.015	0.61	4.34	10.26	0.01	0.06	N.D.	0.011	74.1	0.0	0.0
1776-3	0.084	3.72	0.020	0.011	0.70	5.08	13.35	0.01	0.03	N.D.	0.011	0.5	0.0	0.0
1776-4	0.086	3.36	0.034	0.023	0.43	4.22	11.06	0.03	0.09	N.D.	0.012	57.5	0.0	0.0
1776-5	0.082	3.62	0.018	0.023	0.72	5.04	11.77	0.02	0.04	N.D.	0.013	23.6	0.0	0.0
1777-1	0.098	3.55	0.018	0.013	0.83	14.46	1.73	0.02	0.04	N.D.	0.020	77.2	10.7	11.7
1777-2	0.106	3.11	0.019	0.016	0.82	11.88	1.53	0.02	0.06	N.D.	0.018	79.4	0.3	0.0
1777-3	0.107	3.33	0.027	0.016	0.54	13.77	1.73	0.03	0.06	N.D.	0.020	76.7	5.2	6.7
1777-4	0.112	3.56	0.018	0.022	0.78	15.71	2.07	0.03	0.04	N.D.	0.025	49.5	12.2	13.1
1777-5	0.106	3.32	0.019	0.022	0.89	15.54	2.08	0.03	0.05	N.D.	0.024	52.7	12.5	15.0
1777-6	0.123	4.04	0.020	0.020	0.91	14.99	2.15	0.02	0.05	N.D.	0.026	44.8	6.6	8.2
1786-1	0.125	4.15	0.015	0.011	0.76	10.89	2.26	0.02	0.04	N.D.	0.019	75.3	0.0	0.0
1786-2	0.144	3.94	0.018	0.016	0.69	8.77	1.60	0.02	0.06	N.D.	0.016	80.6	0.0	0.0
1786-3	0.125	3.86	0.017	0.010	0.79	9.76	1.78	0.02	0.05	N.D.	0.019	76.2	0.0	0.0
1787-1	0.089	4.24	0.012	0.017	0.61	5.27	13.33	0.02	0.04	N.D.	0.012	2.5	0.0	0.0
1787-2	0.113	3.15	0.0014	0.019	0.48	3.40	8.98	0.01	0.05	N.D.	0.011	74.2	0.0	0.0
1787-3	0.106	3.41	0.015	0.017	0.57	3.86	10.11	0.01	0.05	N.D.	0.011	77.8	0.0	0.0
1787-4	0.099	3.42	0.014	0.018	0.57	3.96	11.06	0.02	0.05	N.D.	0.011	56.2	0.0	0.0
1791-1	0.082	4.00	0.012	0.014	0.58	4.54	13.48	0.01	0.03	N.D.	0.015	26.1	0.0	0.0
1791-126	0.073	5.40	0.014	0.009	0.73	5.61	17.62	0.01	0.03	N.D.	0.012	0.0	0.0	0.0
1791-128	0.074	4.88	0.015	0.011	0.80	5.18	16.40	0.01	0.03	N.D.	0.012	0.0	0.0	0.0
1791-2	0.101	3.19	0.011	0.017	0.35	2.97	9.60	0.01	0.07	N.D.	0.014	84.0	0.0	0.0
1791-3	0.085	4.58	0.013	0.012	0.63	5.01	15.62	0.01	0.03	N.D.	0.016	0.0	0.0	0.0
1791-4	0.079	4.30	0.013	0.011	0.60	4.60	14.91	0.01	0.03	N.D.	0.015	0.0	0.0	0.0
1792-1	0.115	3.36	0.012	0.011	0.65	15.98	1.57	0.01	0.04	N.D.	0.019	68.9	17.3	16.6
1792-2	0.121	2.79	0.014	0.016	0.41	11.51	1.23	0.01	0.04	N.D.	0.018	81.2	0.0	0.0
1792-3	0.111	3.99	0.011	0.010	0.67	19.15	2.08	0.01	0.03	N.D.	0.022	67.9	76.4	33.3
1792-4	0.109	4.49	0.012	0.011	0.70	20.30	1.94	0.01	0.03	N.D.	0.022	66.8	>100	44.9
1792-5	0.102	4.28	0.012	0.012	0.68	20.26	2.01	0.01	0.03	N.D.	0.025	78.7	>100	48.1
1793-1	0.112	11.66	0.012	0.010	0.80	4.95	6.61	0.02	0.03	N.D.	0.018	0.0	0.0	0.0
1793-2	0.110	9.22	0.010	0.014	0.42	3.51	4.76	0.01	0.05	N.D.	0.012	17.2	0.0	0.0
1793-3	0.101	11.33	0.011	0.010	0.71	4.75	6.35	0.01	0.04	N.D.	0.021	0.0	0.0	0.0
1793-4	0.109	9.31	0.011	0.013	0.54	3.70	4.97	0.01	0.04	N.D.	0.010	11.6	0.0	0.0
1793-5	0.110	9.49	0.011	0.014	0.47	3.63	5.14	0.01	0.05	N.D.	0.012	4.0	0.0	0.0
1793-6	0.103	10.47	0.015	0.010	0.71	4.23	5.68	0.01	0.07	N.D.	0.012	0.1	0.0	0.0
1793-7	0.103	9.78	0.018	0.011	0.76	3.81	5.14	0.01	0.08	N.D.	0.012	4.3	0.0	0.0
1794-1	0.102	11.72	0.015	0.008	0.97	11.25	2.73	0.01	0.05	N.D.	0.025	4.1	0.0	0.0
1794-2	0.099	11.68	0.018	0.008	0.99	10.50	2.70	0.01	0.06	N.D.	0.021	5.7	0.0	0.0
1794-3	0.108	9.21	0.013	0.011	0.77	8.91	2.06	0.01	0.08	N.D.	0.017	12.6	0.0	0.0
1794-4	0.105	8.60	0.019	0.012	0.81	7.47	1.90	0.01	0.08	N.D.	0.016	25.9	0.0	0.0
1794-5	0.111	9.81	0.015	0.013	0.66	8.34	2.15	0.01	0.09	N.D.	0.017	21.6	0.0	0.0
1795-1	0.108	11.04	0.012	0.009	0.80	9.91	3.06	0.01	0.04	0.00	0.020	0.8	0.0	0.0
1795-1R	0.104	11.25	0.013	0.009	0.79	10.77	3.36	0.01	0.03	0.00	0.020	0.7	0.0	0.0
1795-2	0.109	10.36	0.013	0.010	0.63	9.27	2.94	0.01	0.04	0.00	0.018	4.5	0.0	0.0
1795-3	0.111	9.90	0.013	0.016	0.60	8.88	2.77	0.01	0.04	0.00	0.016	9.3	0.0	0.0
1795-4	0.115	9.92	0.013	0.013	0.55	8.58	2.69	0.01	0.04	0.00	0.016	10.2	0.0	0.0
1795-5	0.116	9.38	0.012	0.015	0.49	8.09	2.48	0.01	0.04	0.00	0.015	14.0	0.0	0.0

(a) N.D. = Not Determined.
(b) Some bending before crack.

Table 2 — Continued

Bend	Measured "FN" after bend	WRC-1992 Cr_{eq}	WRC-1992 Ni_{eq}	Schaeffler Cr_{eq}	Schaeffler Ni_{eq}	Wire Feed, in./min	Travel Speed, in./min	Volts DCEP	Amps	Electrical Extension in.	Welding Technique
ok	2.5	9.68	14.48	10.19	15.86	200	20	34	N.D.	1	stringer
ok	21.1	9.01	13.48	9.45	14.54	240	24	34	N.D.	1	stringer
ok	21.0	8.59	13.69	8.97	14.68	280	28	34	N.D.	1	stringer
ok	32.8	7.95	13.14	8.36	14.06	280	28	38	N.D.	1	stringer
ok	35.9	7.86	13.73	8.25	14.79	300	28	40	N.D.	1	stringer
crack	44.9	7.58	12.81	7.96	13.80	320	30	40	N.D.	1	stringer
ok	26.8	8.92	12.73	9.49	13.76	240	8	30	N.D.	1	oscillation
ok	25.7	8.97	13.48	9.58	14.67	280	9	30	490	1	oscillation
ok	22.8	8.85	13.19	9.58	14.39	320	10	30	515	1	oscillation
ok	33.2	15.58	7.72	16.30	8.90	90	12	34	N.D.	1	stringer
ok	42.6	16.18	7.23	16.87	8.58	120	15	34	N.D.	1	stringer
ok	63.8	15.57	7.14	16.23	8.38	150	18	34	N.D.	1	stringer
ok	63.2	15.48	7.01	16.05	8.18	180	21	34	N.D.	1	stringer
crack	80.0	14.61	6.90	15.11	7.97	210	24	34	N.D.	1	stringer
crack	82.2	14.29	6.86	15.12	8.02	180	6	30	370	1	oscillation
crack	82.7	12.69	6.81	13.73	7.91	220	7	30	415	1	oscillation
crack[b]	46.0	11.26	9.84	11.96	10.96	240	8	30	N.D.	1	oscillation
crack	76.7	10.98	9.38	11.69	10.32	280	9	30	N.D.	1	oscillation
crack[b]	83.0	11.74	9.62	12.54	10.49	200	8	30	N.D.	1	oscillation
crack	70.3	11.02	9.83	11.77	10.88	180	7	30	375	1	oscillation
ok	16.3	13.13	10.82	14.13	12.15	160	6	30	355	1	oscillation
crack[b]	53.7	10.87	9.60	11.75	10.52	170	6.5	30	360	1	oscillation
crack[b]	54.6	11.28	9.62	12.19	10.64	165	6	30	345	1	oscillation
ok	33.4	12.33	10.10	13.60	11.25	160	5	30	350	1	oscillation
crack[b]	64.8	4.92	15.58	6.14	16.85	150	4	30	360	1	oscillation
crack	82.5	4.35	13.71	5.27	14.77	200	6.5	30	415	1	oscillation
ok	34.3	5.10	16.51	6.15	17.72	120	4	30	310	1	oscillation
crack[b]	81.7	4.25	14.33	4.90	15.32	130	5	30	340	1	oscillation
crack[b]	43.8	5.06	14.91	6.15	16.04	130	4	30	340	1	oscillation
crack	84.2	14.48	5.57	15.73	6.45	150	4	30	360	1	oscillation
crack	81.0	11.90	5.61	13.13	6.27	200	6.5	30	410	1	oscillation
crack	80.5	13.80	5.89	14.61	6.60	120	4	30	300	1	oscillation
crack	72.0	15.73	6.50	16.90	7.21	100	4	30	340	1	oscillation
crack	69.4	15.57	6.28	16.90	6.91	80	4	30	220	1	oscillation
crack	72.1	15.02	6.99	16.38	7.86	120	4	30	280	1	oscillation
crack	77.0	10.91	7.02	12.05	8.08	100	4	30	270	1	oscillation
crack	81.2	8.79	6.97	9.83	7.89	200	8	30	340	1	oscillation
crack	80.8	9.78	6.54	10.96	7.46	80	4	30	175	1½	oscillation
ok	26.9	5.29	16.69	6.21	18.12	100	4	30	270	1	oscillation
crack	84.2	3.41	13.17	4.13	13.95	200	8	30	435	1	oscillation
crack	86.8	3.88	14.05	4.73	14.99	150	6	30	375	1	oscillation
crack	77.6	3.98	14.76	4.84	15.74	125	5	30	345	1	oscillation
crack[b]	65.9	4.55	16.66	5.43	17.94	100	4	30	295	1	oscillation
ok	0.0	5.62	20.43	6.71	22.51	100	4	26	N.D.	1	oscillation
ok	0.4	5.19	19.24	6.38	21.06	100	4	28	265	1	oscillation
crack	86.1	2.98	13.44	3.50	14.23	200	8	30	465	1	oscillation
ok	0.3	5.02	18.92	5.97	20.46	100	4	30	250	1½	oscillation
ok	11.5	4.61	17.99	5.50	19.43	100	4	30	265	1¼	oscillation
crack	76.9	15.99	5.98	16.96	6.70	100	4	30	285	1	oscillation
crack	81.7	11.52	5.83	12.13	6.25	200	8	30	445	1	oscillation
crack[b]	69.7	19.17	6.41	20.16	7.40	100	4	30	240	1½	oscillation
crack[b]	66.6	20.30	6.20	21.35	7.45	100	4	30	210	2	oscillation
crack[b]	77.6	20.27	6.09	21.29	7.21	100	4	30	245	1¼	oscillation
ok	11.1	4.97	10.90	6.17	15.80	100	4	30	265	1	oscillation
crack[b]	65.8	3.52	8.86	4.15	12.67	200	8	30	425	1	oscillation
ok	12.8	4.76	10.31	5.82	15.05	125	5	30	315	1	oscillation
crack[b]	55.2	3.71	9.00	4.52	12.90	150	6	30	365	1	oscillation
crack[b]	56.7	3.64	9.24	4.35	13.18	175	7	30	390	1	oscillation
ok	31.5	4.24	9.55	5.30	14.01	150	6	28	355	1	oscillation
crack[b]	50.2	3.82	9.00	4.95	13.12	175	7	28	390	1	oscillation
crack[b]	34.5	11.26	6.82	12.72	11.65	100	4	28	265	1	oscillation
crack[b]	50.2	10.51	6.60	12.00	11.51	125	5	28	315	1	oscillation
crack	50.9	8.91	6.20	10.07	9.90	150	6	28	330	1	oscillation
crack	45.4	7.47	5.91	8.69	9.35	175	7	28	360	1	oscillation
crack	61.7	8.35	6.39	9.34	10.38	200	8	28	395	1	oscillation
ok	30.0	9.92	7.25	11.13	11.82	100	4	28	295	1	oscillation
ok	23.6	10.78	7.41	11.98	12.10	100	4	28	295	1	oscillation
crack[b]	38.6	9.28	7.12	10.22	11.39	125	5	28	345	1	oscillation
ok	50.9	8.89	6.98	9.78	11.05	150	6	28	370	1	oscillation
crack[b]	53.6	8.59	7.05	9.41	11.10	175	7	28	400	1	oscillation
crack[b]	64.4	8.10	6.85	8.83	10.65	200	8	28	445	1	oscillation

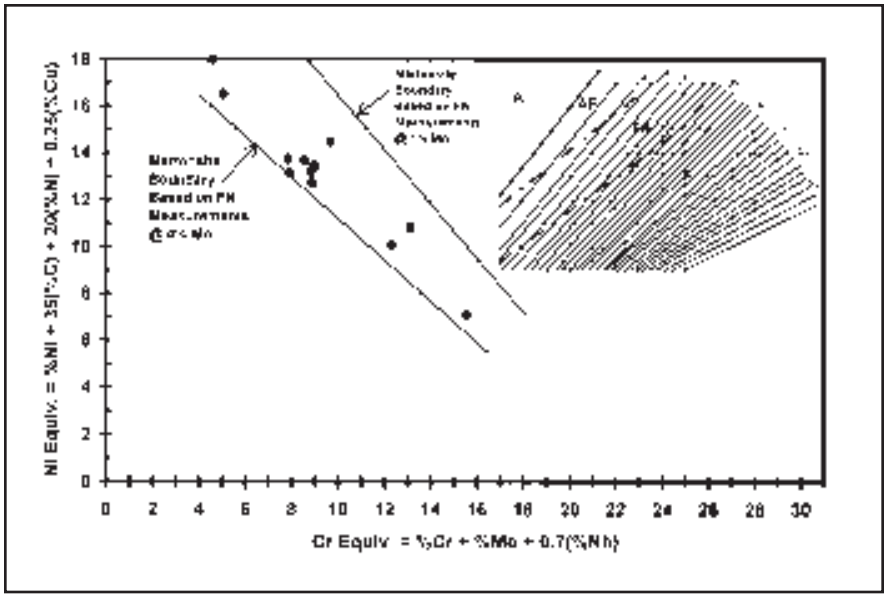

Fig. 2 — Martensite-free 4% Mn compositions on the WRC-1992 Diagram. Many 4% Mn compositions, indicated by solid circles, are below and left of the 1% Mn martensite-free boundary. A 4% Mn martensite-free boundary, based on magnetic measurements, is indicated.

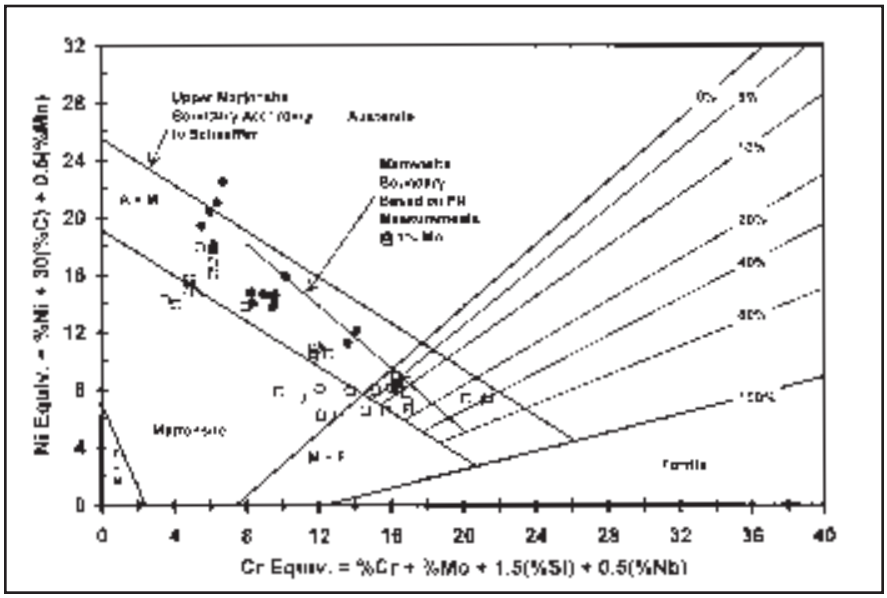

Fig. 3 — Bend/break results at 4% Mn on the Schaeffler Diagram. Compositions that passed the 2T bend test are shown as solid circles. Compositions that cracked during bending are shown as open squares.

ted on the diagrams in two ways. First, only compositions whose measured "FN" was less than the calculated FN plus 1 were plotted on each diagram to find the lower left boundary of such compositions. Then, all the results were plotted on each diagram, with a different symbol for those that passed the bend test than for those that cracked, in order to find a boundary dividing the two types of bend test behavior.

Experimental Results

Table 2 lists all the experimental weld compositions in this phase of the study, along with the welding conditions employed in making each weld, calculated nickel and chromium equivalents, 2T longitudinal face bend test results, and measured "FN" before and after bending. In many cases, the measured "FN" after bending is much higher than before bending, which indicates considerable transformation of austenite to martensite during bending, which is to be expected. It is the presence or absence of martensite before bending that is of interest. More than 50 compositions were examined at the nominal level of 4% Mn, and 18 were examined at the nominal level of 10% Mn.

4% Mn Compositions

Figure 1 plots the magnetically determined martensite-free 4% Mn compositions, from Table 2, on the Schaeffler Diagram. No lower left boundary for martensite-free compositions is offered for 4% Mn compositions because it is not the intent to propose a correction to the Schaeffler Diagram. Despite the fact the Schaeffler Diagram includes manganese in the nickel equivalent, it can be qualitatively seen that, for 4% Mn, the magnetically determined limit of martensite-free compositions has shifted leftward and somewhat counterclockwise relative to the 1% Mn boundary observed in Part 1 of this study.

Figure 2 plots the same composition data on the WRC-1992 Diagram. A boundary line for 4% Mn compositions is indicated in this figure. Without manganese in the nickel equivalent, the leftward and counterclockwise shift of the magnetically determined martensite boundary from 1 to 4% Mn is more pronounced in this diagram than in the Schaeffler Diagram.

Figure 3 plots the bend test results on the Schaeffler Diagram. As was noted in the first part of this study where 1% Mn compositions were considered, there is a transition region of mixed pass-fail results. Above and to the right of this mixed zone, all compositions, except three very high in ferrite, pass the 2T bend test. The failure of the high ferrite compositions to pass the bend test can be attributed to excessive ferrite, not to martensite. In a study of duplex ferritic-austenitic stainless steel weld metals, it was found (Ref. 8) that ferrite above 60 FN resulted in reduced ductility in the weld metal, so this is not unexpected. Below and to the left of this mixed bend test zone, all compositions fail the 2T bend test. Again, the magnetically determined martensite boundary lies within the zone of mixed bend test results.

Figure 4 plots these same bend test results on the WRC-1992 Diagram. Compositions in the upper right portion of the diagram all bent, except for the three high ferrite compositions, as noted above. These three compositions are calculated, by extrapolating the iso-ferrite lines of the WRC-1992 Diagram, to have

more than 75 FN each. Compositions in the lower left portion of the diagram all broke. And there is a transition zone, indicated by a pair of heavy parallel lines, of mixed behavior in bending. The magnetically determined martensite boundary is within this transition zone. This zone of mixed bending behavior is shifted leftward and rotated counterclockwise from the similar zone for 1% Mn compositions, as determined in the first part of this study.

10% Mn Compositions

Figure 5 plots the magnetically determined martensite-free compositions of nominally 10% Mn on the Schaeffler Diagram. Further leftward shift of martensite-free compositions can be seen as compared to 4% and 1% Mn compositions. In particular, a composition can be seen that is entirely martensite-free but lies within the region of the Schaeffler Diagram predicted to be completely martensite. Clearly, the Schaeffler Diagram is inadequate for predicting martensite in these high manganese compositions.

Figure 6 plots the magnetically determined martensite-free 10% Mn compositions on the WRC-1992 Diagram, with a lower-left boundary for such compositions. It should be noted there are not a lot of compositions available to act as a basis for this boundary, so there must be considerable uncertainty attached to it. However, leftward shift and counterclockwise rotation of the boundary compared to that for the 4% and 1% Mn compositions is evident.

Figure 7 plots the 2T bend test data at 10% Mn on the Schaeffler Diagram. As in the case of the 4% Mn results, there is no attempt to draw boundaries for compositions that all bend, or all break, because there is no intention to propose a correction to the Schaeffler Diagram. It can be noted there are two compositions in the zone predicted by the diagram to consist of 100% martensite that passed the bend test.

Figure 8 plots the 2T bend test data at 10% Mn on the WRC-1992 Diagram. Once again, there is a transition zone, indicated by heavy parallel lines, of mixed bend test behavior, and the magnetically determined martensite-free boundary lies within this zone of mixed bend test behavior. Compositions above and to the right of this transition zone all bend. Compositions below and to the left of this transition zone all break during the bend test. A further leftward shift and counterclockwise rotation of the transition zone, as compared to that for 4% Mn, is evident.

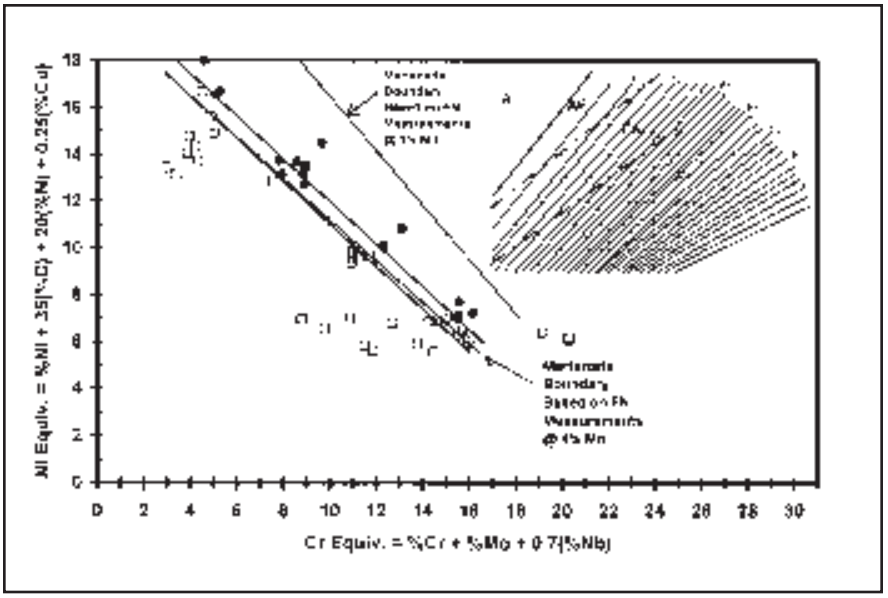

Fig. 4 — Bend/break results at 4% Mn on the WRC-1992 Diagram. Compositions that passed the 2T bend test are shown as solid circles. Compositions that cracked during bending are shown as open squares. Between the two parallel heavy lines, some compositions bent and some cracked. Above and to the right of these two lines, all compositions bent, except for a few very high ferrite compositions. Below and to the left of these two lines, all compositions cracked in bending.

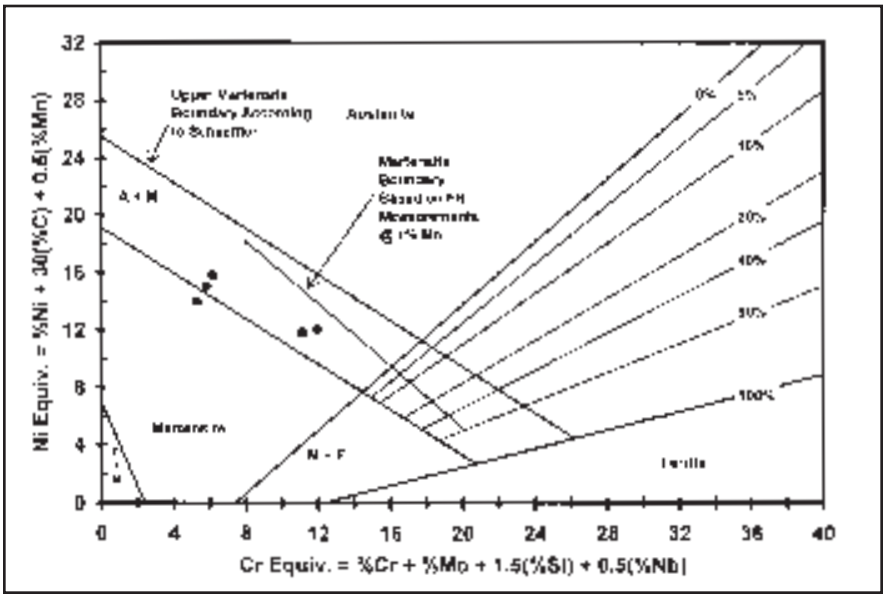

Fig. 5 — Martensite-free 10% Mn compositions on the Schaeffler Diagram. Note one of these compositions is within the area considered to be 100% martensite according to the diagram, but it is martensite-free.

Discussion of Results

Three levels of manganese have been considered in stainless steel weld deposits. The 1% Mn level, from the previous part of this study, is normal for most common austenitic stainless steel weld claddings. The 4% Mn level, considered herein, might be encountered when producing buffer layers using 18 8 Mn or 307 filler metal. And the 10% Mn level might be encountered when using stainless steel filler metals high in manganese (the AWS 200 series filler metals). In all three cases, the Schaeffler Diagram has been shown to predict martensite in compositions that were magnetically determined to be martensite-free, and which pass the 2T bend test. The disagreement between the Schaeffler predictions and the exper-

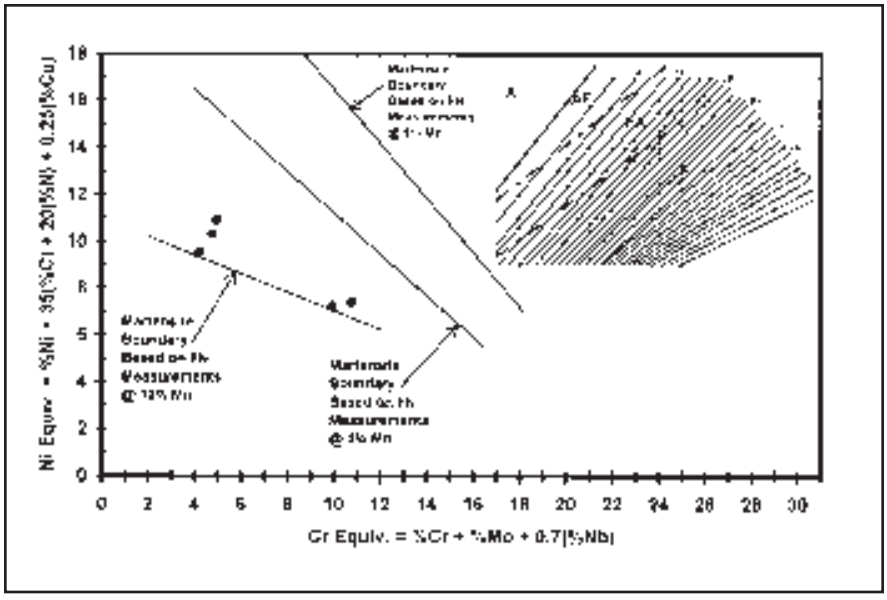

Fig. 6 — Martensite-free 10% Mn compositions on the WRC-1992 Diagram. Many 10% Mn compositions, indicated by solid circles, are below and left of the 4% Mn boundary obtained by magnetic measurements. A 10% Mn martensite-free boundary is indicated.

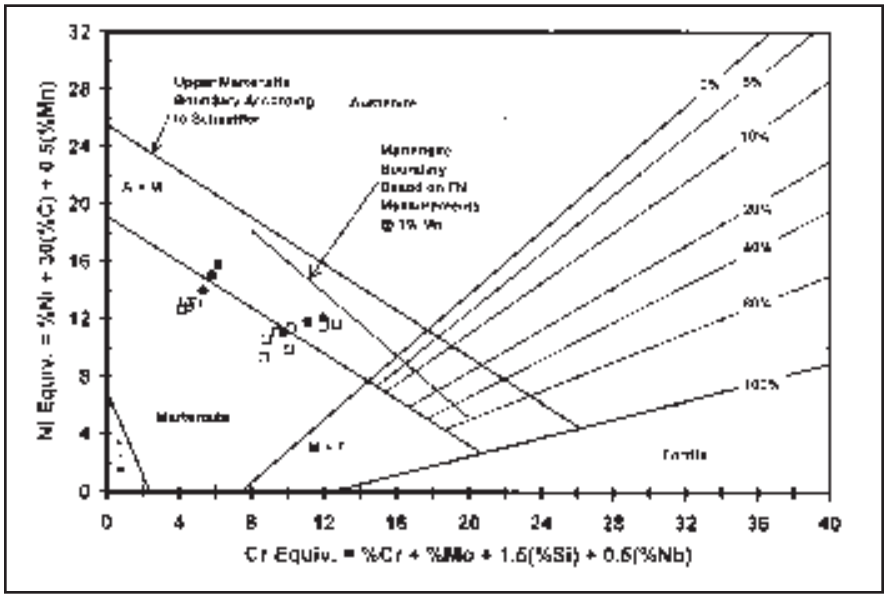

Fig. 7 — Bend/break results at 10% Mn on the Schaeffler Diagram. Compositions that passed the 2T bend test are shown as solid circles. Compositions that cracked are shown as open squares.

imental results becomes greater at higher manganese levels.

There is no reason to expect that manganese should have exactly the same effect (weighting factor relative to nickel) on martensite formation at low temperatures as it has on ferrite formation at high temperatures. The Schaeffler Diagram, with a coefficient of 0.5 for Mn in the Nickel Equivalent, proposes that Mn is both half as powerful as Ni in stabilizing austenite with respect to ferrite formation at high temperatures, and half as powerful as Ni in stabilizing austenite relative to martensite formation at low temperatures. The WRC-1992 Diagram does not include manganese in the Nickel Equivalent at all, which means that manganese has no effect on ferrite formation at high temperatures. So the way is clear to provide different martensite boundaries for different manganese levels. These are shown in Fig. 9 as shaded zones. Each shaded boundary zone includes the magnetically determined martensite-free boundary and the lines bounding the extremes of the transition zone between bend and break behavior in the 2T bend test.

The three shaded boundary zones, corresponding to three manganese levels, are each drawn with parallel sides as a practical matter. If the sides were not parallel, the edges would cross at some point, which is absurd from a realistic point of view. The uncertainty associated with the width of each shaded zone is considered to be due mainly to uncertainty in chemical analysis. If a single sample of weld metal is analyzed repeatedly, on successive days, the results reported from one day to the next for each element will vary. Then the calculated chromium equivalent and nickel equivalent will vary as well. So one cannot say with certainty what the exact chromium equivalent and nickel equivalent are for a given weld sample. This uncertainty is reflected in the width of the shaded boundary zone. In the case of the 10% manganese compositions, there are fewer data points, so the uncertainty (shaded boundary width) is indicated to be greater than that for the other two manganese levels.

The strength of manganese relative to that of nickel, with respect to stabilizing austenite against transformation to martensite, can be estimated from the vertical displacement of the martensite boundary obtained by increasing the Mn content from 1 to 4%. It can be seen from Fig. 9 that this vertical displacement due to the additional 3% Mn amounts to about 4 nickel equivalent near the right end of the 4% Mn martensite boundary (*i.e.*, at a chromium equivalent of 16). This would mean a coefficient for manganese in the nickel equivalent of about 1.3 (4 nickel equivalent divided by 3% Mn) at 16% Cr. Near the left end of the 1% Mn martensite boundary (*i.e.*, at a chromium equivalent of 10), the vertical displacement due to the additional 3% Mn amounts to about 5 nickel equivalent. This would mean a coefficient for manganese in the nickel equivalent of about 1.7 (5 nickel equivalent divided by 3% Mn) at 10% Cr. So manganese is more powerful than nickel in stabilizing austenite with respect to transformation to martensite, not half as powerful as proposed by the Schaeffler Diagram, and the power of manganese increases with decreasing chromium content.

The observed leftward shifting and counterclockwise rotation of the martensite boundary as the manganese content increases is not really surprising. Self, *et al.* (Ref. 7), predicted this shifting and rotation graphically, based upon the equations of Andrews (Ref. 9). Self, *et al.,* pro-

pose a coefficient for manganese in the Nickel Equivalent with respect to austenite transformation to martensite that increases with decreasing chromium content, as given in Equation 1 below.

$$\text{Coefficient for Mn} = 1/(0.083x\%Cr + 0.5) \quad (1)$$

The prediction of Self, *et al.* Ref. 7), can be tested against the observed shift in the martensite boundary. At 16% Cr, Equation 1 proposes the coefficient for Mn to be 0.547, vs. the observed value of 1.3. And at 10% Cr, Equation 1 proposes the coefficient to be 0.752, vs. the observed value of 1.7. There appears, therefore, to be qualitative agreement between the predictions of Self, *et al*., in that the coefficient for manganese increases with decreasing chromium content. However, there is not quantitative agreement — the observed coefficients are about 2.3 times as large as predicted by Self, *et al.* (Ref. 7).

In a later review of microstructure prediction in austenitic stainless steel weld metal, Olson (Ref. 10) reproduces a martensite-start temperature relationship from Self, *et al.* (Ref. 11), that indicates manganese to be 1.7 times as powerful as nickel in stabilizing austenite, which is much more consistent with the 1.3 to 1.7 factor observed herein.

It must be recognized there is a degree of uncertainty in the exact location of the martensite boundary at any manganese level. At all three manganese levels examined, this degree of uncertainty is indicated by presenting the martensite boundary as a shaded zone. This shaded boundary zone is on the order of 1.5 chromium equivalent, or 1.5 nickel equivalent, wide (more in the case of the 10% Mn level). Above and to the right of each martensite boundary zone, all compositions at the given manganese level are martensite-free in the as-welded condition, and these compositions pass a 2T bend test unless they contain excessive ferrite. Below and to the left of each martensite boundary zone, all compositions at the given manganese level contain martensite in the as-deposited condition and fail a 2T bend test. Within the shaded martensite boundary zone, the behavior is unpredictable.

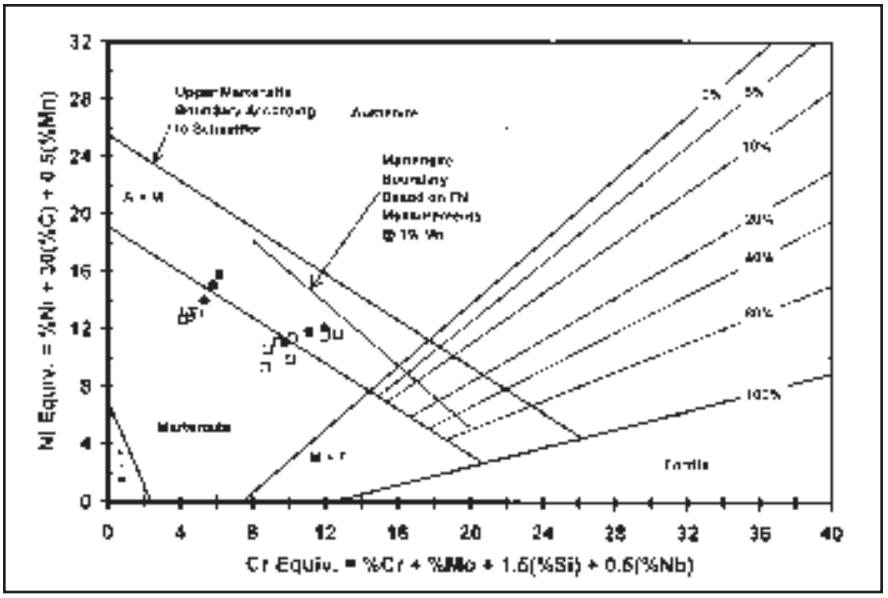

Fig. 8 — Bend/break results at 10% Mn on the WRC-1992 Diagram. Compositions that passed the 2T bend test are shown as solid circles. Compositions that cracked during bending are shown as open squares. Between the two parallel heavy lines, some compositions bent and some cracked. Above and to the right of the heavy lines, all compositions bent. Below and to the left of the heavy lines, all compositions cracked in bending.

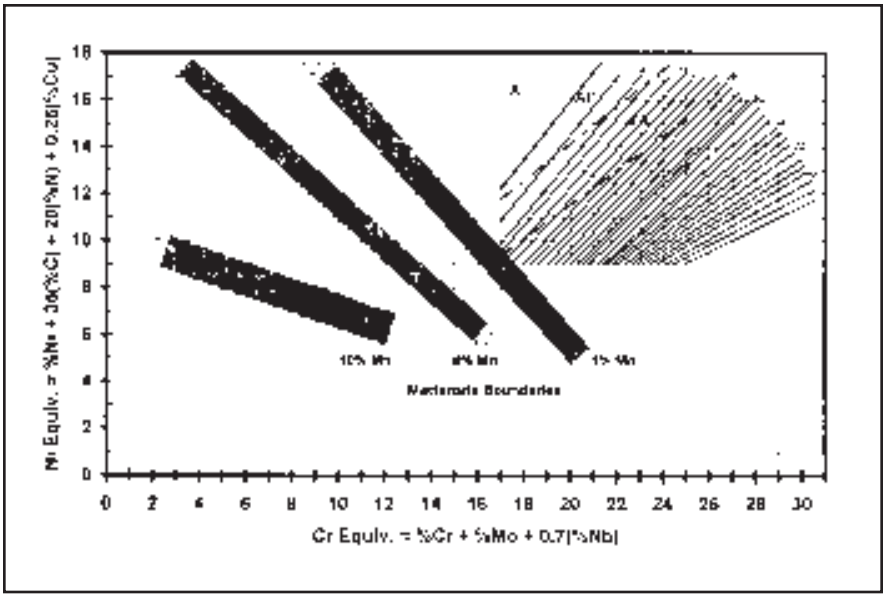

Fig. 9 — The WRC-1992 Diagram, with martensite boundaries for 1, 4 and 10% Mn. The boundaries are shown as shaded bands to indicate a degree of uncertainty in their positions. Each boundary includes the extreme of martensite-free compositions as determined by magnetic measurements, and the limits of mixed bend/break behavior in the 2T bend test.

Conclusions

An experimentally determined modification of the WRC-1992 Diagram has been developed, as shown in Fig. 9. This now provides the possibility to predict whether or not stainless steel clad layers, over nonalloy or low-alloy steels, will be free of martensite and will pass a 2T bend test. With the modified WRC-1992 Diagram, the graphical methods used for predicting ferrite in cladding or dissimilar metal joining (Ref. 3) can now be applied also to predicting martensite.

Future Work

Part 3 of this study will examine the effects of carbon, nitrogen and molybdenum on the position of the martensite boundary in the WRC-1992 Diagram.

Acknowledgments

The author is grateful to The Lincoln Electric Co. for the opportunity to pursue this interest and for the laboratory sup-

port necessary. Bill Spang was especially helpful in preparing the test welds and extracting test pieces.

References

1. Schaeffler, A. L. 1949. Constitution diagram for stainless steel weld metal. *Metal Progress* 56(11): 680 to 680B.

2. DeLong, W. T. 1974. Ferrite in austenitic stainless steel weld metal. *Welding Journal* 53(7): 273-s to 286-s.

3. Kotecki, D. J., and Siewert, T. A. 1992. WRC-1992 constitution diagram for stainless steel weld metals: a modification of the WRC-1988 diagram. *Welding Journal* 71(5): 171-s to 178-s.

4. *ASME Boiler and Pressure Vessel Code*, 1995 Edition, Section III, Division I, Figure NB-2433.1-1. The American Society of Mechanical Engineers, N.Y.

5. Kotecki, D. J. 1999. A martensite boundary on the WRC-1992 Diagram. *Welding Journal* 78(5): 180-s to 192-s.

6. Szumachowski, E. R., and Kotecki, D. J. 1984. Effect of manganese on stainless steel weld metal ferrite. *Welding Journal* 63(5):156-s to 161-s.

7. Self, J. A., Matlock, D. K., and Olson, D. L. 1984. An evaluation of austenitic Fe-Mn-Ni weld metal for dissimilar metal welding. *Welding Journal* 63(9): 282-s to 288-s.

8. Kotecki, D. J. 1986. Ferrite control in duplex stainless steel weld metal. *Welding Journal* 65(10): 273-s to 278-s.

9. Andrews, K. 1965. Empirical formulae for the calculation of some transformation temperatures. *JISI* 203: 721 to 727.

10. Olson, D. L. 1985. Prediction of austenitic weld metal microstructure and properties. *Welding Journal* 64(10): 281-s to 295-s.

11. Self, J. A., Olson, D. L., and Edwards, G. R. July 1984. The stability of austenitic weld metal. *Proc. of IMCC*, Kiev, Ukraine.

Preparation of Manuscripts for Submission to the *Welding Journal* Research Supplement

All authors should address themselves to the following questions when writing papers for submission to the Welding Research Supplement:

- Why was the work done?
- What was done?
- What was found?
- What is the significance of your results?
- What are your most important conclusions?

With those questions in mind, most authors can logically organize their material along the following lines, using suitable headings and subheadings to divide the paper.

1) **Abstract.** A concise summary of the major elements of the presentation, not exceeding 200 words, to help the reader decide if the information is for him or her.

2) **Introduction.** A short statement giving relevant background, purpose and scope to help orient the reader. Do not duplicate the abstract.

3) **Experimental Procedure, Materials, Equipment.**

4) **Results, Discussion.** The facts or data obtained and their evaluation.

5) **Conclusion.** An evaluation and interpretation of your results. Most often, this is what the readers remember.

6) **Acknowledgment, References and Appendix.**

Keep in mind that proper use of terms, abbreviations and symbols are important considerations in processing a manuscript for publication. For welding terminology, the *Welding Journal* adheres to ANSI/AWS A3.0-94, *Standard Welding Terms and Definitions.*

Papers submitted for consideration in the Welding Research Supplement are required to undergo Peer Review before acceptance for publication. Submit an original and one copy (double-spaced, with 1-in. margins on 8 ½ x 11-in. or A4 paper) of the manuscript. Submit the abstract only on a computer disk. The preferred format is from any Macintosh® word processor on a 3.5-in. double- or high-density disk. Other acceptable formats include ASCII text, Windows™ or DOS. A manuscript submission form should accompany the manuscript.

Tables and figures should be separate from the manuscript copy and only high-quality figures will be published. Figures should be original line art or glossy photos. Special instructions are required if figures are submitted by electronic means. To receive complete instructions and the manuscript submission form, please contact the Peer Review Coordinator, Doreen Kubish, at (305) 443-9353, ext. 275; FAX 305-443-7404; or write to the American Welding Society, 550 NW LeJeune Rd., Miami, FL 33126.